

HyperKon: A Self-Supervised Contrastive Network for Hyperspectral Image Analysis

Daniel L Ayuba

Belen Marti-Cardona

Jean-Yves Guillemaut

Oscar Mendez Maldonado
University Of Surrey

{d.ayuba, b.marti-cardona, j.guillemaut, o.mendez}@surrey.ac.uk

Abstract

The exceptional spectral resolution of hyperspectral imagery enables material insights that are not possible with RGB or multispectral images. Yet, the full potential of this data is often underutilized by deep learning techniques due to the scarcity of hyperspectral-native CNN backbones. To bridge this gap, we introduce HyperKon, a self-supervised contrastive learning network designed and trained on hyperspectral data from the EnMAP Hyperspectral Satellite [31]. HyperKon uniquely leverages the high spectral continuity, range, and resolution of hyperspectral data through a spectral attention mechanism and specialized convolutional layers. We also perform a thorough ablation study on different kinds of layers, showing their performance in understanding hyperspectral layers. It achieves an outstanding 98% Top-1 retrieval accuracy and outperforms traditional RGB-trained backbones in hyperspectral pan-sharpening tasks. Additionally, in hyperspectral image classification, HyperKon surpasses state-of-the-art methods, indicating a paradigm shift in hyperspectral image analysis and underscoring the importance of hyperspectral-native backbones.

1. Introduction

Hyperspectral Images (HSIs), with their ability to capture detailed spectral information across hundreds of contiguous bands, have rapidly advanced the capabilities of remote sensing analysis in various domains, including agriculture, mineralogy, and environmental monitoring [6, 12]. This high-dimensional data offers a rich representation of scenes, enabling finer material distinctions than traditional RGB and multispectral images [14]. However, the exploitation of HSI, particularly using deep learning techniques initially designed for RGB images, presents considerable challenges [63].

Convolutional Neural Networks (CNNs) which dom-

inate the computer vision landscape, are predominantly trained and evaluated on RGB data [50]. These models often struggle to generalize effectively to hyperspectral data due to the vast difference in spectral resolution and the unique characteristics of hyperspectral images [5, 49, 50]. Moreover, the scarcity of native hyperspectral backbones necessitates extensive fine-tuning for their application in this domain.

While Transformers have shown promise in various computer vision tasks [7, 16, 67], their application to hyperspectral data is not without challenges. Transformers, which are primarily designed for global feature extraction, may not adequately capture the local spectral-spatial nuances fundamental in hyperspectral images, and their high computational requirements and the requirement for a large amount of training data frequently make them less feasible for hyperspectral applications, particularly in scenarios with limited data availability [24].

Deep learning, leveraging both spatial and spectral data, has shown exceptional performance in hyperspectral image tasks such as classification [63], segmentation [37], object detection [13], and unmixing [58]. Despite this, the reliance on RGB-trained backbones in hyperspectral research implies a lack of full exploitation of the spectral potential, often leading to domain adaptation issues [45].

To address these limitations and the scarcity of hyperspectral-specific solutions, we introduce HyperKon, a novel self-supervised contrastive network trained exclusively on HSIs from Environmental Mapping and Analysis Program (EnMAP). HyperKon, distinct from generic CNN backbones, is designed to fully harness the unique properties of hyperspectral data, presenting an innovative approach in hyperspectral image analysis.

The main contributions of this paper are:

1. HyperKon: a hyperspectral-native CNN backbone that can learn useful representations from large amounts of unlabelled data.

2. EnHyperSet-1: An EnMAP dataset curated for use in precision agriculture and other deep learning projects.
3. HyperSpectral Perceptual Loss: A perceptual loss function emphasizing minimizing errors in the spectral domain.
4. Demonstration that the representations learned by HyperKon improve performance in hyperspectral downstream tasks.

2. Related Work

2.1. Hyperspectral Sensors

Recent advances in hyperspectral sensors stem from the rising demand for intricate spectral details in areas like remote sensing, environmental monitoring, and sustainable agriculture. These sensors allow for in-depth examination of the chemical and physical characteristics of objects, especially important in agriculture where reflected radiation from plants is important.

The EnMAP project by the German Aerospace Center (DLR), introduced in 2022, boasts a cutting-edge hyperspectral sensor catering to diverse applications, from agriculture to mineral exploration [31]. Covering wavelengths from 420 nm to 2450 nm, its imager delivers high-resolution spectral data with pixel sizes of 30m by 30m of the Earth’s surface. Public access to EnMAP data has paved the way for AI-driven in-depth analyses.

Anticipated satellite missions, like the Copernicus Hyperspectral Imaging Mission for the Environment (CHIME) by the European Space Agency (ESA) scheduled for 2028, aim to elevate hyperspectral imaging by capturing over 400 spectral bands [40]. These advancements highlight the growing need for advanced computer vision techniques tailored to hyperspectral data.

2.2. Deep Learning for Hyperspectral Analysis

Deep learning, particularly through the use of CNNs and attention mechanisms like Transformers, has significantly advanced HSI applications. These techniques have improved performance in classification [35], segmentation [39], denoising [56], and spatial resolution enhancement.

HSI Classification and Segmentation: Early works like [27] demonstrated the superior accuracy of CNNs over traditional algorithms in HSI classification. Innovations in network architectures, such as those introduced by [34], incorporating global pooling layers and channel attention mechanisms, have furthered this progress, yielding competitive results on benchmarks [18, 42].

Enhancing Spatial Resolution: The inherent challenge of low spatial resolution in hyperspectral images, due to constraints in spaceborne sensors [1], has led to advancements in Hyperspectral Super-Resolution (HSR) and pan-

sharpening techniques. Techniques ranging from ResNet-based approaches [19] to multiscale CNNs [25] and combinations of variational autoencoders with deep residual networks [11] have been developed. These advancements are crucial for improving the spatial resolution of HSI, thereby enhancing the performance of downstream tasks.

The Need for Hyperspectral-Native Solutions: However, a notable gap in the field is the reliance on RGB-trained backbones for these methods [38, 66]. Such backbones may not fully capture the unique spectral details crucial in hyperspectral data, especially in applications requiring fine spectral discrimination.

2.3. RGB-Backbones vs. Hyperspectral-Native Approaches in Deep Learning

The Role of CNNs and Transformers: CNNs have been foundational in image analysis, demonstrating their capability in tasks like classification [2, 35], object detection [68], and more [57]. The success of CNNs is largely attributed to their robust feature extraction backbones, as seen in models like VGG [52], ResNet [20], and DenseNet [29]. Parallel to CNNs, attention mechanisms such as Transformers have gained traction in computer vision, exemplified by the Vision Transformers (ViT) [16], which offers comparable performance to CNN-based models in image recognition.

Transformers in Hyperspectral Classification: Transformers have shown promise in hyperspectral data classification, capturing global spectral-spatial features effectively. Examples include the spatial-spectral transformer network [22] and other models utilizing self-attention mechanisms for hyperspectral classification [17, 28].

Our Focus and Contribution: Despite the advancements in both CNNs and Transformers, our research is oriented towards leveraging the strengths of CNNs for developing hyperspectral-native solutions. We chose CNNs due to their proven effectiveness in processing and recognizing complex spatial hierarchies in multi-dimensional data, a key requirement for hyperspectral image analysis [24]. Furthermore, the parameter efficiency and adaptability of CNNs make them well-suited for handling the vast spectral diversity inherent in hyperspectral data [63]. In this context, we propose HyperKon, a CNN-based network specifically designed to harness the rich spectral information in hyperspectral images. HyperKon aims to address the critical gap in hyperspectral-native deep learning architectures, offering enhanced capabilities for applications like precision agriculture, where recognizing subtle spectral differences is crucial.

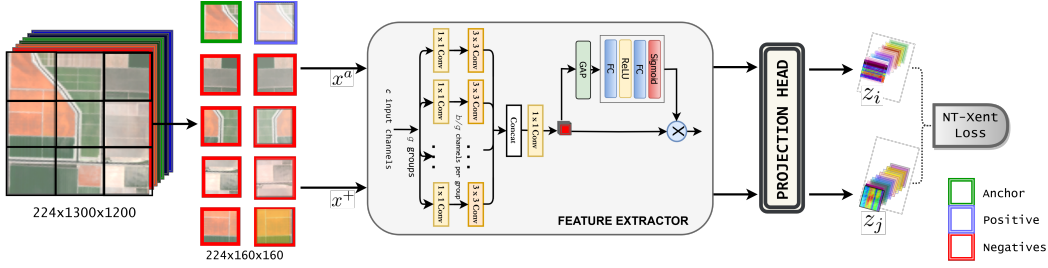


Figure 1. General Overview of HyperKon System Architecture

3. Methodology

3.1. Hyperspectral Backbone Architecture

The HyperKon network architecture as shown in Figure 1 is designed to effectively handle the complexity and high dimensionality inherent in hyperspectral data. Influenced by the principle of multibranch cardinality, the network is configured into multiple parallel paths, optimizing representational power and computational efficiency. This technique, central to the ResNeXt architecture [59], strikes a balance between enhancing representational capability and ensuring computational efficiency, particularly beneficial for data with substantial dimensional depth, like hyperspectral images. Furthermore, as depicted in Figure 2, the ResNeXt architecture has fewer parameters, making it have reduced sensitivity to learning rates and other hyper-parameters, especially when compared to its predecessor, ResNet [20]. Developing an effective feature ex-

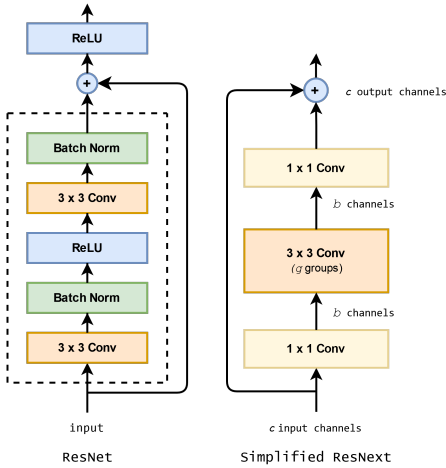


Figure 2. Comparison of ResNet and ResNeXt architectures

tractor for this network requires overcoming two main challenges: capturing the complex, high-dimensional spectral, and spatial features of hyperspectral data and addressing the computational constraints associated with such high-dimensional data.

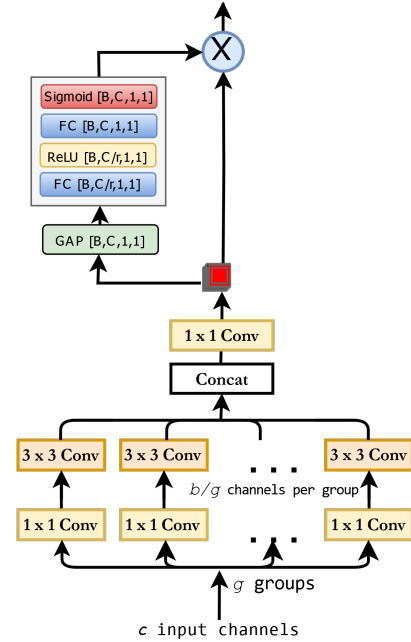


Figure 3. The Feature Extractor used in HyperKon

In the case of Hyperspectral imagery, it is desirable to recalibrate feature maps so that they model channel interdependencies. In our architecture, this is achieved by a novel SEB-based architecture, shown in figure 3. Given an input feature map $X \in \mathbb{R}^{H \times W \times C}$, the squeeze operation computes channel-wise statistics. It enhances the network's ability to distill and prioritize spectral and spatial information from the high-dimensional data, thus ensuring that the computational resources are optimally utilized. The excitation operation then uses a gating mechanism:

$$s_c = \frac{1}{H \times W} \sum_{i=1}^H \sum_{j=1}^W x_{ijc}, \quad (1)$$

$$e_c = \sigma(\beta \cdot s_c + \gamma),$$

where σ is the sigmoid activation, and β and γ are trainable parameters. The recalibrated feature map $X' \in \mathbb{R}^{H \times W \times C}$

is given by:

$$x'_{ijc} = e_c \cdot x_{ijc} \quad (2)$$

This recalibration emphasizes channels with high interdependencies and suppresses others. The feature extractor provides preliminary feature representations which, while powerful, might not be fine-tuned to the specific challenges presented by hyperspectral data. To address this, we introduce a projection head. Given the deep feature representation $F \in \mathbb{R}^D$ from the feature extractor, the projection head transforms it into a new space $Z \in \mathbb{R}^{D'}$:

$$Z = W_2 \sigma(W_1 F + b_1) + b_2 \quad (3)$$

where $W_1 \in \mathbb{R}^{D' \times D}$, $W_2 \in \mathbb{R}^{D' \times D'}$, $b_1 \in \mathbb{R}^{D'}$, and $b_2 \in \mathbb{R}^{D'}$ are trainable parameters, and σ is a non-linear activation function. This transformation aids in emphasizing discriminative features for hyperspectral data. Having established the architectural foundation, we now focus on the learning approach that leverages the power of this architecture.

3.2. Contrastive Learning

The refined model uses the NT-Xent [10] loss function, enhancing its ability to learn distinct features and proving valuable for various hyperspectral image analyses.

3.2.1 Self-supervised contrastive loss:

The complexity of hyperspectral data demanded a versatile loss function capable of handling its high dimensionality and suitable for smaller batch sizes. While Triplet loss [48] and Info-NCE [41] can be effective, they require meticulous sample selection, especially challenging for hyperspectral data due to its spectral domain variance. NT-Xent loss [10], however, is adaptable to varying batch sizes, uses cosine similarity for feature vector orientation, and performs well with high-dimensional data, making it the ideal choice for HyperKon. The NT-Xent loss is defined as:

$$\ell_{(z_i, z_j)} = -\frac{1}{N} \sum_{i=1}^N \log \frac{\exp(\text{sim}(z_i, z_{i'})/\tau)}{\sum_{j=1}^{2N} \exp(\text{sim}(z_i, z_j)/\tau)} \quad (4)$$

where N is the number of samples, z_i is the feature representation of sample i , $\text{sim}(z_i, z_j) = z_i^T z_j$ is the cosine similarity between z_i and z_j , τ is a temperature parameter that controls the smoothness of the distribution, and $z_{i'}$ refers to the positive feature representation for the query sample i .

3.2.2 HSI Contrastive Sampling:

Self-supervised contrastive learning heavily leans on the use of image augmentation to extract valuable features from the input data [44]. Yet, standard augmentation techniques

commonly employed for RGB images [30] don't have a specific equivalent explicitly designed for HSI. Let's denote $x_i \in I_k^h$ as a sequence of patches (x_i) taken from a series of hyperspectral images ($I_k^h \forall k = 0 \dots S$) where S represents the dataset size. These patches can then be subjected to a sequence of transformations $A = a_1, a_2 \dots a_n$, which are enacted on the patches x_i as follows:

$$x'_i = a_n(\dots a_2(a_1(x_i))\dots) \quad (5)$$

During the selection of triplet pairs, the hard negative pairs method [47] is implemented to pick negative pairs within the same batch. This method aids in choosing negative samples that pose a difficulty to distinguish from the positive samples, thereby enhancing the contrastive learning experience.

The mathematical formulation for selecting hard negative pairs within a batch is as follows:

Let's denote f as the encoder function that takes an input patch x and produces the corresponding embedding $z = f(x)$. Provided a batch of B patches x_1, x_2, \dots, x_B , the embeddings z_1, z_2, \dots, z_B can be computed using the encoder function. The cosine similarity between the embeddings z_i and z_j is measured by the similarity function $s(z_i, z_j)$, which is used to select the hard negative pairs. Therefore, for a specific anchor patch x^a and its positive pair x^+ , a hard negative pair x^- is sampled by:

$$x^- = \underset{x_k \in \{x_1, x_2, \dots, x_B\} \setminus \{x^a, x^+\}}{\text{argmax}} s(f(x^a), f(x_k)) \quad (6)$$

This means, the patch x_k that gives the highest similarity

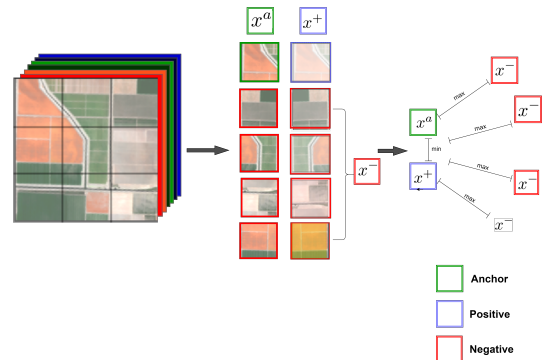


Figure 4. Illustration of HSI Contrastive sampling

score with the anchor patch x^a is chosen from all patches in the batch, with the exception of the positive pair x^+ and the anchor patch x^a itself (as depicted in Figure 4). Overall, this approach underscores the significance of selecting suitable data augmentation techniques for HSI and brings to the forefront the potential advantages of utilizing self-supervised contrastive learning to derive meaningful representations from HSI data.

Table 1. A comparison to popular hyperspectral datasets. *

Dataset	Number of Bands	Size	Spectral Range	Number of Images	Spatial Resolution	Imaging Location	Platform Type
Indian Pines	200	145x145	400-2500nm	1	30m	Indiana, USA	Airborne
Pavia Centre	102	1096x1096	430-860nm	1	1.3m	Pavia, Italy	Airborne
Salinas	204	512x217	360-2500nm	1	3.7m	Salinas Valley, California, USA	Airborne
Harvard	31	1392x1040	420-720nm	50	-	Harvard, USA	Airborne
Botswana	145	1476x256	400-2500nm	1	30m	Botswana	Airborne
Chikusei	100	2517x2335	263-1018nm	1	2.5m	Chikusei, Japan	Airborne
EnHyperSet-1	224	1276x1248	420-2450nm	800	30m	Global, on demand	Spaceborne

* Color Convention: **best**

4. Results

4.1. Experimental setup

4.1.1 Dataset

The study employs a specialized dataset named EnHyperSet-1, tailored for hyperspectral deep learning applications. Sourced from the EnMAP portal, the dataset includes 800 images of size 1,300 by 1,200 pixels, providing over 8,100 samples, segregated into distinct levels [8]: Level 1B, Level 1C, and Level 2A. Level 1B images present radiometrically corrected radiance measurements. Level 1C images are an orthorectified version of Level 1B, with geolocation assigned to each pixel. Meanwhile, Level 2A images build upon Level 1C by making atmospheric corrections for aspects like gas absorption and aerosol scattering and calculating the reflectance values for each pixel. Each high-resolution hyperspectral image pixel represents a 30m x 30m terrestrial section. The spectral resolution ranges from 6.5 nm to 12 nm, spanning from 420 nm to 2450 nm.

The EnHyperSet-1 dataset stands out for its expansive spectral range, fine spectral resolution, and optimal patch dimensions, as highlighted in Table 1. The 160x160 pixel patches balance spatial detail capture and efficient processing. Featuring diverse scenes, including urban, forest, and agricultural settings, EnHyperSet-1, though recent, has demonstrated its efficacy in training algorithms, evident from HyperKon’s performance when trained on it.

The HyperKon network was pretrained on EnHyperSet-1 using self-supervised contrastive learning with the NT-Xent loss. The training dataset comprised a diverse set of hyperspectral patches measuring 160 x 160 pixels, with a 5% overlap from various scenes, including urban, agricultural, and natural landscapes. The network was trained for a total of 10,000 epochs with a batch size of 32, using the Adam optimizer with an initial learning rate of 1e-4 and a Stepped learning rate scheduler.

4.1.2 Ablation Study

After pretraining, the HyperKon network was evaluated using Top-K nearest neighbour retrieval accuracy to assess feature representation capabilities from hyperspectral data.

Higher accuracy suggests successful capture of essential spectral and spatial hyperspectral characteristics, beneficial for tasks such as classification or segmentation.

The results, as depicted in Figure 5, confirm the effectiveness of HyperKon in representing hyperspectral data features. This highlights its potential in hyperspectral image analysis and its role in enhancing the performance of deep learning models in areas like precision agriculture, environmental monitoring, and land cover classification. The findings also emphasize the importance of designing CNN backbones specifically for hyperspectral data, which offer better performance than traditional RGB-Native backbones.

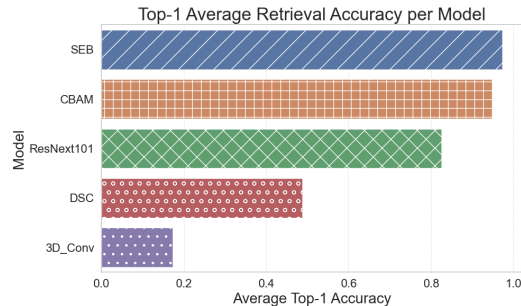


Figure 5. This showcases the top-1 HSI retrieval accuracy achieved by various versions of the HyperKon model during the pretraining phase. The performance of each version is presented as a bar in the chart, illustrating how the integration of different components, such as 3D convolutions, DSC, the CBAM, and the SEB, affected the model’s accuracy. The chart underscores the superior performance of SEB.

4.1.3 Band Attention

We conducted another study focusing on dimensionality reduction techniques which are commonly applied to this type of data [32, 36, 65]. Principal Component Analysis (PCA), Manual, and Full Band Selection were among the methods investigated. Dimensionality reduction is critical in hyperspectral image processing because it not only streamlines computation but also has the potential to refine the feature extraction or transfer learning process by discarding redundant information. Contrary to our initial expectations, as shown in Figure 6, the 3D Conv model outperformed both the Squeeze and Excitation Block (SEB) and Convolutional Block Attention Module (CBAM) models when dimension-

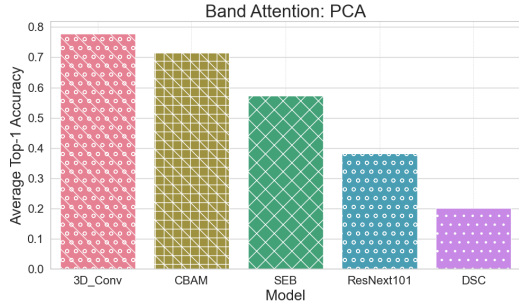


Figure 6. Top-1 HSI retrieval accuracy for the 3D Conv, SEB, and CBAM models following dimensionality reduction using PCA. The graph indicates a superior performance by the 3D Conv model.

ality was reduced using PCA. SEB and CBAM generally demonstrate their proficiency by effectively selecting and prioritising information across the entire spectrum of hyperspectral bands; however, their advantage appears to diminish when PCA is used, potentially rendering their roles redundant. With the ability to attend to locally contiguous channels, 3D convolutions demonstrate superior performance when band selection is conducted *a priori* using PCA with 112 components. As suggested in Figure 7, manual band selection gives 3D convolutions a distinct advantage. However, most notably, SEB and CBAM clearly surpass 3D convolution when no band selection is carried out. In these circumstances, 3D convolution is at a disadvantage due to its constraint of only attending to locally contiguous channels. This observation confirms our hypothesis: in the absence of *a priori* band selection, attention mechanisms have the capacity to attend across the entire channel spectrum outperform those with more limited range. Further analy-

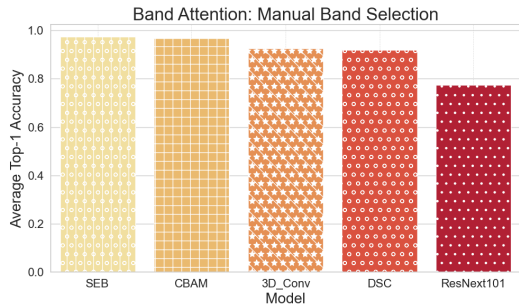


Figure 7. Top-1 HSI retrieval accuracy for the 3D Conv, SEB, and CBAM models when manual band selection is employed. It shows an initial advantage for 3D Conv, but over time, the SEB and CBAM models catch up to similar levels of performance.

sis revealed that the SEB and CBAM model variants performed optimally without the application of PCA. See Figure 7. This clearly demonstrates their robustness and ability to manage the high dimensionality inherent in hyperspectral data.

4.2. Super Resolution

For the super-resolution evaluation, we utilized datasets such as EnMAP and Pavia, each featuring different spectral bands. Specific bands from the EnHyperSet-1 dataset were selected to match the wavelength of each dataset, optimizing the training of HyperKon. This tailored approach aimed to enhance the super-resolution outcomes. The data preparation adhered to methodologies outlined in [4] and [69].

The results from HyperKon were benchmarked against traditional RGB-trained backbones using metrics [9, 15, 53] such as Correlation Coefficient (CC), Spectral Angle Mapper (SAM), Root Mean Square Error (RMSE), Erreur Relative Globale Adimensionnelle de Synthèse (ERGAS), and Peak Signal-to-Noise Ratio (PSNR). This setup ensured a balanced comparison and highlighted the potential of HyperKon in a variety of hyperspectral tasks.

4.2.1 HyperKon as a Perceptual Loss Network

We evaluated the use of HyperKon as a perceptual loss network for hyperspectral deep learning downstream tasks, comparing its performance to traditional RGB-trained backbones. See Table 2 and 3. Specifically, we focused on tasks such as hyperspectral image super-resolution. Our experiments demonstrated that using HyperKon as a perceptual loss network led to improved performance in these tasks compared to using RGB-trained backbones. This is primarily because HyperKon was specifically designed and trained for hyperspectral data, allowing it to capture more relevant features and better supervise the deep learning models in these tasks.

Table 2. Average quantitative results: Pavia Center [43]. *

Pavia Center Dataset					
Method	CC \uparrow	SAM \downarrow	RMSE \downarrow	ERGAS \downarrow	PSNR \uparrow
HySure [51]	0.966	6.13	1.8	3.77	35.91
HyperPNN [21]	0.967	6.09	1.67	3.82	36.7
PanNet [61]	0.968	6.36	1.83	3.89	35.61
Darn [69]	0.969	6.43	1.56	3.95	37.3
HyperKite [4]	0.98	5.61	1.29	2.85	38.65
SIPSA [33]	0.948	5.27	2.38	4.52	33.65
GPPNN [60]	0.963	6.52	1.91	4.05	35.36
HyperTransformer [3]	<u>0.9881</u>	<u>4.1494</u>	<u>0.9862</u>	<u>0.5346</u>	<u>40.9525</u>
Ours	0.9883	3.9551	0.9369	0.5152	41.9808

* Color Convention: **first**, second, third. RMSE values are $\times 10^{-2}$

Table 3. A comparison of the average quantitative pansharpening results*

Metric	Botswana Dataset		Chikusei Dataset		Pavia Dataset	
	RGB-Native	HS-Native	RGB-Native	HS-Native	RGB-Native	HS-Native
CC \uparrow	0.9104	0.9411	0.9801	0.9777	0.9881	0.9883
SAM \downarrow	3.1459	2.5798	2.2547	2.4192	4.1494	3.9551
RMSE \downarrow	0.0233	0.0193	0.0123	0.0131	0.0098	0.0093
ERGAS \downarrow	0.6753	0.5249	0.8662	0.9193	0.5346	0.5152
PSNR \uparrow	27.3925	29.4128	36.8861	36.2889	40.9525	41.9808

* Color convention: **Best**

In summary, our experimental results showed that the

HyperKon network, pretrained using self-supervised contrastive learning on EnMAP HSI, was highly effective as a hyperspectral native CNN backbone and as a perceptual loss network for hyperspectral deep learning downstream tasks. These results highlight the potential of the HyperKon network for a wide range of applications in hyperspectral image analysis, paving the way for future research and development in this field

Table 4. Average Classification accuracies of different methods on Hyperspectral Image Classification

Datasets	Metrics	SSAN [54]	SSRN [70]	RvT [23]	HiT [62]	SSFTT [55]	QSSPN-3 [64]	HyperKon
IP	OA(%)	89.46	91.85	83.85	90.59	96.35	95.87	98.77
	AA(%)	85.99	81.51	79.67	86.71	89.99	96.40	97.82
	Kappa(%)	88.04	90.73	81.68	89.27	95.82	95.34	98.60
PU	OA(%)	99.15	99.63	97.37	99.43	99.52	99.71	99.89
	AA(%)	98.70	99.29	95.86	99.09	99.20	99.43	99.76
	Kappa(%)	98.87	99.51	96.52	99.24	99.36	99.61	99.86
SA	OA(%)	98.92	99.31	98.11	99.38	99.53	99.66	99.99
	AA(%)	99.33	99.70	98.83	99.70	99.72	99.81	99.98
	Kappa(%)	98.80	99.23	97.90	99.31	99.47	99.63	99.99

* Color convention: **Best**, **2nd Best**

4.3. Transfer Learning Capability of HyperKon

In addition to the super-resolution task, the performance of the HyperKon network was evaluated on the hyperspectral image classification task using the Indian Pines, Pavia University, and Salinas Scene [46] dataset. This dataset, covering a wide range of crops, serves as an excellent benchmark for assessing the accuracy and proficiency of the HyperKon network in classifying different crops. The frozen backbone of the HyperKon network, which had been pretrained on a variety of hyperspectral data, was utilized for this task

The results were juxtaposed with those of established methods such as SSAN [54], SSRN [70], RvT [23], HiT [62], SSFTT [55], and QSSPN [64]. The assessment utilized overall accuracy (OA), average accuracy (AA), and Kappa coefficient (Kappa) metrics. As shown in Table 4, HyperKon consistently matched or surpassed other networks, highlighting its robustness and adaptability to new data. The commendable accuracy underscores the model’s ability to harness discriminative features from its self-supervised learning phase, leading to accurate predictions in hyperspectral image classification.

5. Discussion

The comparative analysis in Table 3 demonstrates HyperKon’s proficiency in hyperspectral super-resolution, validated against traditional RGB models on datasets including EnMAP, Botswana, Chikusei, and Pavia. Metrics like CC, SAM, RMSE, ERGAS, and PSNR were used for evaluation. HyperKon’s design, which incorporates SEB [26], is pivotal in its superior performance by enhancing band-specific information processing capabilities.

Although HyperKon showed exceptional results, its performance on the Chikusei dataset was not optimal compared to an RGB-Native model. This suggests potential improvements through training on a more diverse set of hyperspectral images to enhance its generalization capacity.

Additionally, HyperKon’s capability for transfer learning was highlighted through its performance in hyperspectral classification tasks, as detailed in Table 4. Its self-supervised pretraining on hyperspectral data allows for effective feature extraction even with limited labeled data, making it a robust tool for applications where acquiring extensive labeled datasets is impractical or expensive.

6. Conclusions

In this study, we introduced HyperKon, a self-supervised contrastive network specifically tailored for hyperspectral image processing. Through rigorous training on a substantial dataset consisting of 8,180 patches of HSIs, HyperKon demonstrated exceptional performance in two critical downstream tasks: hyperspectral super-resolution and image classification, particularly in the context of crop mapping. Our findings highlight the significant potential of self-supervised contrastive networks in hyperspectral image processing and lay a robust foundation for future research in this rapidly expanding field.

Acknowledgement: The author’s of this paper wish to extend their profound gratitude to **Sixteen Sands Ltd** for funding this research work, and the **German Aerospace Center (DLR)** for providing EnMAP free of charge.

References

- [1] Telmo Adão, Jonáš Hruška, Luís Pádua, José Bessa, Emanuel Peres, Raul Morais, and Joaquim Joao Sousa. Hyperspectral imaging: A review on uav-based sensors, data processing and applications for agriculture and forestry. *Remote sensing*, 9(11):1110, 2017. 2
- [2] Carlos Affonso, André Luis Debiaso Rossi, Fábio Henrique Antunes Vieira, André Carlos Ponce de Leon Ferreira, et al. Deep learning for biological image classification. *Expert systems with applications*, 85:114–122, 2017. 2
- [3] Wele Gedara Chaminda Bandara and Vishal M Patel. Hypertransformer: A textural and spectral feature fusion transformer for pansharpening. In *Proceedings of the IEEE/CVF Conference on Computer Vision and Pattern Recognition*, pages 1767–1777, 2022. 6
- [4] Wele Gedara Chaminda Bandara, Jeya Maria Jose Valanarasu, and Vishal M Patel. Hyperspectral pansharpening based on improved deep image prior and residual reconstruction. *IEEE Transactions on Geoscience and Remote Sensing*, 60:1–16, 2021. 6
- [5] Rached Bouchoucha, Housseem Ben Braiek, Foutse Khomh, Sonia Bouzidi, and Rania Zaatour. Robustness assessment of hyperspectral image cnns using metamorphic testing. *Information and Software Technology*, page 107281, 2023. 1
- [6] B Brisco, RJ Brown, T Hirose, H McNairn, and K Staenz. Precision agriculture and the role of remote sensing: a review. *Canadian Journal of Remote Sensing*, 24(3):315–327, 1998. 1
- [7] Zhaowei Cai, Avinash Ravichandran, Paolo Favaro, Manchen Wang, Davide Modolo, Rahul Bhotika, Zhuowen Tu, and Stefano Soatto. Semi-supervised vision transformers at scale. *Advances in Neural Information Processing Systems*, 35:25697–25710, 2022. 1
- [8] German Space Operation Center. Enmap ground segment. 2023. 5
- [9] CC Chaithra, NL Taranath, LM Darshan, and CK Subbaraya. A survey on image fusion techniques and performance metrics. In *2018 Second International Conference on Electronics, Communication and Aerospace Technology (ICECA)*, pages 995–999. IEEE, 2018. 6
- [10] Ting Chen, Simon Kornblith, Mohammad Norouzi, and Geoffrey Hinton. A simple framework for contrastive learning of visual representations. In *International conference on machine learning*, pages 1597–1607. PMLR, 2020. 4
- [11] Wenjing Chen, Xiangtao Zheng, and Xiaoqiang Lu. Hyperspectral image super-resolution with self-supervised spectral-spatial residual network. *Remote Sensing*, 13(7):1260, 2021. 2
- [12] Cheng Cheng and Bo Zhao. Prospect of application of hyperspectral imaging technology in public security. In *International Conference on Applications and Techniques in Cyber Security and Intelligence ATCI 2018: Applications and Techniques in Cyber Security and Intelligence*, pages 299–304. Springer, 2019. 1
- [13] Koushikey Chhapariya, Krishna Mohan Buddhiraju, and Anil Kumar. Cnn-based salient object detection on hyperspectral images using extended morphology. *IEEE Geoscience and Remote Sensing Letters*, 19:1–5, 2022. 1
- [14] Miguel Jorge da Lomba Magalhães. Hyperspectral image fusion—a comprehensive review. Master’s thesis, Itä-Suomen yliopisto, 2022. 1
- [15] Hilda Deborah, Noël Richard, and Jon Yngve Hardeberg. A comprehensive evaluation of spectral distance functions and metrics for hyperspectral image processing. *IEEE Journal of Selected Topics in Applied Earth Observations and Remote Sensing*, 8(6):3224–3234, 2015. 6
- [16] Alexey Dosovitskiy, Lucas Beyer, Alexander Kolesnikov, Dirk Weissenborn, Xiaohua Zhai, Thomas Unterthiner, Mostafa Dehghani, Matthias Minderer, Georg Heigold, Sylvain Gelly, et al. An image is worth 16x16 words: Transformers for image recognition at scale. *arXiv preprint arXiv:2010.11929*, 2020. 1, 2
- [17] Kuiliang Gao, Bing Liu, Zhixiang Xue, Xibing Zuo, Yifan Sun, Mofan Dai, et al. Deep transformer network for hyperspectral image classification. *Academic Journal of Computing & Information Science*, 4(7):11–17, 2021. 2
- [18] Agrim Gupta, Piotr Dollar, and Ross Girshick. Lvis: A dataset for large vocabulary instance segmentation. In *Proceedings of the IEEE/CVF conference on computer vision and pattern recognition*, pages 5356–5364, 2019. 2
- [19] Xian-Hua Han and Yen-Wei Chen. Deep residual network of spectral and spatial fusion for hyperspectral image super-resolution. In *2019 IEEE Fifth International Conference on Multimedia Big Data (BigMM)*, pages 266–270. IEEE, 2019. 2
- [20] Kaiming He, Xiangyu Zhang, Shaoqing Ren, and Jian Sun. Deep residual learning for image recognition. In *Proceedings of the IEEE conference on computer vision and pattern recognition*, pages 770–778, 2016. 2, 3
- [21] Lin He, Jiawei Zhu, Jun Li, Antonio Plaza, Jocelyn Chanussot, and Bo Li. Hyperpnn: Hyperspectral pansharpening via spectrally predictive convolutional neural networks. *IEEE Journal of Selected Topics in Applied Earth Observations and Remote Sensing*, 12(8):3092–3100, 2019. 6
- [22] Xin He, Yushi Chen, and Zhouhan Lin. Spatial-spectral transformer for hyperspectral image classification. *Remote Sensing*, 13(3):498, 2021. 2
- [23] Byeongho Heo, Sangdoo Yun, Dongyoon Han, Sanghyuk Chun, Junsuk Choe, and Seong Joon Oh. Rethinking spatial dimensions of vision transformers. In *Proceedings of the IEEE/CVF International Conference on Computer Vision*, pages 11936–11945, 2021. 7
- [24] Danfeng Hong, Zhu Han, Jing Yao, Lianru Gao, Bing Zhang, Antonio Plaza, and Jocelyn Chanussot. Spectralformer: Rethinking hyperspectral image classification with transformers. *IEEE Transactions on Geoscience and Remote Sensing*, 60:1–15, 2021. 1, 2
- [25] Jianwen Hu, Pei Hu, Xudong Kang, Hui Zhang, and Shaosheng Fan. Pan-sharpening via multiscale dynamic convolutional neural network. *IEEE Transactions on Geoscience and Remote Sensing*, 59(3):2231–2244, 2020. 2
- [26] Jie Hu, Li Shen, and Gang Sun. Squeeze-and-excitation networks. In *Proceedings of the IEEE conference on computer vision and pattern recognition*, pages 7132–7141, 2018. 7

- [27] Wei Hu, Yangyu Huang, Li Wei, Fan Zhang, and Hengchao Li. Deep convolutional neural networks for hyperspectral image classification. *Journal of Sensors*, 2015:1–12, 2015. 2
- [28] Xin Huang, Mengjie Dong, Jiayi Li, and Xian Guo. A 3-d-swin transformer-based hierarchical contrastive learning method for hyperspectral image classification. *IEEE Transactions on Geoscience and Remote Sensing*, 60:1–15, 2022. 2
- [29] Forrest Iandola, Matt Moskewicz, Sergey Karayev, Ross Girshick, Trevor Darrell, and Kurt Keutzer. Densenet: Implementing efficient convnet descriptor pyramids. *arXiv preprint arXiv:1404.1869*, 2014. 2
- [30] Ashish Jaiswal, Ashwin Ramesh Babu, Mohammad Zaki Zadeh, Debapriya Banerjee, and Fillia Makedon. A survey on contrastive self-supervised learning. *Technologies*, 9(1):2, 2020. 4
- [31] Hermann Kaufmann, Karl Segl, Theres Kuester, Christian Roga, Stefan Hofer, Andreas Mueller, and Christian Chlebek. The environmental mapping and analysis program (enmap). In *IEEE Int. Geoscience and Remote Sensing Symp.*, 2012. 1, 2
- [32] Brajesh Kumar, Onkar Dikshit, Ashwani Gupta, and Manoj Kumar Singh. Feature extraction for hyperspectral image classification: A review. *International Journal of Remote Sensing*, 41(16):6248–6287, 2020. 5
- [33] Jaehyup Lee, Soomin Seo, and Munchurl Kim. Sipsa-net: Shift-invariant pan sharpening with moving object alignment for satellite imagery. In *Proceedings of the IEEE/CVF Conference on Computer Vision and Pattern Recognition*, pages 10166–10174, 2021. 6
- [34] Ruirui Li, Wenjie Liu, Lei Yang, Shihao Sun, Wei Hu, Fan Zhang, and Wei Li. Deepunet: A deep fully convolutional network for pixel-level sea-land segmentation. *IEEE journal of selected topics in applied earth observations and remote sensing*, 11(11):3954–3962, 2018. 2
- [35] Shutao Li, Weiwei Song, Leyuan Fang, Yushi Chen, Pedram Ghamisi, and Jon Atli Benediktsson. Deep learning for hyperspectral image classification: An overview. *IEEE Transactions on Geoscience and Remote Sensing*, 57(9):6690–6709, 2019. 2
- [36] Wei Li, Fubiao Feng, Hengchao Li, and Qian Du. Discriminant analysis-based dimension reduction for hyperspectral image classification: A survey of the most recent advances and an experimental comparison of different techniques. *IEEE Geoscience and Remote Sensing Magazine*, 6(1):15–34, 2018. 5
- [37] Li Liu, Emad Mahrous Awwad, Yasser A Ali, Muna Al-Razgan, Ali Maarouf, Laith Abualigah, and Azadeh Noori Hoshyar. Multi-dataset hyper-cnn for hyperspectral image segmentation of remote sensing images. *Processes*, 11(2):435, 2023. 1
- [38] Laetitia Loncan, Luis B De Almeida, José M Bioucas-Dias, Xavier Briottet, Jocelyn Chanussot, Nicolas Dobigeon, Sophie Fabre, Wenzhi Liao, Giorgio A Licciardi, Miguel Simoes, et al. Hyperspectral pansharpening: A review. *IEEE Geoscience and remote sensing magazine*, 3(3):27–46, 2015. 2
- [39] Shervin Minaee, Yuri Y Boykov, Fatih Porikli, Antonio J Plaza, Nasser Kehtarnavaz, and Demetri Terzopoulos. Image segmentation using deep learning: A survey. *IEEE transactions on pattern analysis and machine intelligence*, 2021. 2
- [40] Jens Nieke and Michael Rast. Towards the copernicus hyperspectral imaging mission for the environment (chime). In *Igarss 2018-2018 ieee international geoscience and remote sensing symposium*, pages 157–159. IEEE, 2018. 2
- [41] Aaron van den Oord, Yazhe Li, and Oriol Vinyals. Representation learning with contrastive predictive coding. *arXiv preprint arXiv:1807.03748*, 2018. 4
- [42] Federico Perazzi, Jordi Pont-Tuset, Brian McWilliams, Luc Van Gool, Markus Gross, and Alexander Sorkine-Hornung. A benchmark dataset and evaluation methodology for video object segmentation. In *Proceedings of the IEEE conference on computer vision and pattern recognition*, pages 724–732, 2016. 2
- [43] Antonio Plaza, Jon Atli Benediktsson, Joseph W Boardman, Jason Brazile, Lorenzo Bruzzone, Gustavo Camps-Valls, Jocelyn Chanussot, Mathieu Fauvel, Paolo Gamba, Anthony Gualtieri, et al. Recent advances in techniques for hyperspectral image processing. *Remote sensing of environment*, 113:S110–S122, 2009. 6
- [44] Senthil Purushwalkam and Abhinav Gupta. Demystifying contrastive self-supervised learning: Invariances, augmentations and dataset biases. *Advances in Neural Information Processing Systems*, 33:3407–3418, 2020. 4
- [45] Aneesh Prasad Rangnekar. *Learning Representations in the Hyperspectral Domain in Aerial Imagery*. Rochester Institute of Technology, 2022. 1
- [46] Charles M Sarture Thomas G Chrien Mikael Aronsson Bruce J Chippendale Jessica A Faust Betina E Pavri Christopher J Chovit Manuel Solis Martin R Olah Robert O Green, Michael L Eastwood and Orlesa Williams. Imaging spectroscopy and the airborne visible/infrared imaging spectrometer (aviris). *Remote Sensing of Environment*, 65(3):227–248, 1998. 7
- [47] Joshua Robinson, Ching-Yao Chuang, Suvrit Sra, and Stefanie Jegelka. Contrastive learning with hard negative samples. *arXiv preprint arXiv:2010.04592*, 2020. 4
- [48] Florian Schroff, Dmitry Kalenichenko, and James Philbin. Facenet: A unified embedding for face recognition and clustering. In *Proceedings of the IEEE conference on computer vision and pattern recognition*, pages 815–823, 2015. 4
- [49] Cuiping Shi, Jingwei Sun, and Liguang Wang. Hyperspectral image classification based on spectral multiscale convolutional neural network. *Remote Sensing*, 14(8):1951, 2022. 1
- [50] Alberto Signoroni, Mattia Savardi, Annalisa Baronio, and Sergio Benini. Deep learning meets hyperspectral image analysis: A multidisciplinary review. *Journal of Imaging*, 5(5):52, 2019. 1
- [51] Miguel Simoes, José Bioucas-Dias, Luis B Almeida, and Jocelyn Chanussot. A convex formulation for hyperspectral image superresolution via subspace-based regularization. *IEEE Transactions on Geoscience and Remote Sensing*, 53(6):3373–3388, 2014. 6

- [52] Karen Simonyan and Andrew Zisserman. Very deep convolutional networks for large-scale image recognition. *arXiv preprint arXiv:1409.1556*, 2014. 2
- [53] Arvind Kumar Singh, HV Kumar, Govind R Kadambi, JK Kishore, James Shuttleworth, and J Manikandan. Quality metrics evaluation of hyperspectral images. *The International Archives of the Photogrammetry, Remote Sensing and Spatial Information Sciences*, 40:1221–1226, 2014. 6
- [54] Hao Sun, Xiangtao Zheng, Xiaoqiang Lu, and Siyuan Wu. Spectral–spatial attention network for hyperspectral image classification. *IEEE Transactions on Geoscience and Remote Sensing*, 58(5):3232–3245, 2019. 7
- [55] Le Sun, Guangrui Zhao, Yuhui Zheng, and Zebin Wu. Spectral–spatial feature tokenization transformer for hyperspectral image classification. *IEEE Transactions on Geoscience and Remote Sensing*, 60:1–14, 2022. 7
- [56] Chunwei Tian, Lunke Fei, Wenxian Zheng, Yong Xu, Wangmeng Zuo, and Chia-Wen Lin. Deep learning on image denoising: An overview. *Neural Networks*, 131:251–275, 2020. 2
- [57] Athanasios Voulodimos, Nikolaos Doulamis, Anastasios Doulamis, Eftychios Protopapadakis, et al. Deep learning for computer vision: A brief review. *Computational intelligence and neuroscience*, 2018, 2018. 2
- [58] Jie Wang, Jindong Xu, Qianpeng Chong, Zhaowei Liu, Weiqing Yan, Haihua Xing, Qianguo Xing, and Mengying Ni. Ssanet: An adaptive spectral–spatial attention autoencoder network for hyperspectral unmixing. *Remote Sensing*, 15(8):2070, 2023. 1
- [59] Peida Wu, Ziguan Cui, Zongliang Gan, and Feng Liu. Three-dimensional resnext network using feature fusion and label smoothing for hyperspectral image classification. *Sensors*, 20(6):1652, 2020. 3
- [60] Shuang Xu, Jiangshe Zhang, Zixiang Zhao, Kai Sun, Junmin Liu, and Chunxia Zhang. Deep gradient projection networks for pan-sharpening. In *Proceedings of the IEEE/CVF Conference on Computer Vision and Pattern Recognition*, pages 1366–1375, 2021. 6
- [61] Junfeng Yang, Xueyang Fu, Yuwen Hu, Yue Huang, Xinghao Ding, and John Paisley. Pannet: A deep network architecture for pan-sharpening. In *Proceedings of the IEEE international conference on computer vision*, pages 5449–5457, 2017. 6
- [62] Xiaofei Yang, Weijia Cao, Yao Lu, and Yicong Zhou. Hyperspectral image transformer classification networks. *IEEE Transactions on Geoscience and Remote Sensing*, 60:1–15, 2022. 7
- [63] Shiqi Yu, Sen Jia, and Chunyan Xu. Convolutional neural networks for hyperspectral image classification. *Neurocomputing*, 219:88–98, 2017. 1, 2
- [64] Jie Zhang, Yongshan Zhang, and Yicong Zhou. Quantum-inspired spectral-spatial pyramid network for hyperspectral image classification. In *Proceedings of the IEEE/CVF Conference on Computer Vision and Pattern Recognition*, pages 9925–9934, 2023. 7
- [65] Liangpei Zhang and Fulin Luo. Review on graph learning for dimensionality reduction of hyperspectral image. *Geospatial Information Science*, 23(1):98–106, 2020. 5
- [66] Meilin Zhang, Xiongli Sun, Qiqi Zhu, and Guizhou Zheng. A survey of hyperspectral image super-resolution technology. In *2021 IEEE International Geoscience and Remote Sensing Symposium IGARSS*, pages 4476–4479. IEEE, 2021. 2
- [67] Pengchuan Zhang, Xiyang Dai, Jianwei Yang, Bin Xiao, Lu Yuan, Lei Zhang, and Jianfeng Gao. Multi-scale vision longformer: A new vision transformer for high-resolution image encoding. In *Proceedings of the IEEE/CVF international conference on computer vision*, pages 2998–3008, 2021. 1
- [68] Zhong-Qiu Zhao, Peng Zheng, Shou-tao Xu, and Xindong Wu. Object detection with deep learning: A review. *IEEE transactions on neural networks and learning systems*, 30(11):3212–3232, 2019. 2
- [69] Yuxuan Zheng, Jiaojiao Li, Yunsong Li, Jie Guo, Xianyun Wu, and Jocelyn Chanussot. Hyperspectral pan-sharpening using deep prior and dual attention residual network. *IEEE transactions on geoscience and remote sensing*, 58(11):8059–8076, 2020. 6
- [70] Zilong Zhong, Jonathan Li, Zhiming Luo, and Michael Chapman. Spectral–spatial residual network for hyperspectral image classification: A 3-d deep learning framework. *IEEE Transactions on Geoscience and Remote Sensing*, 56(2):847–858, 2017. 7